Design and Analysis of High-Speed Permanent Magnet Synchronous Generator With Rotor Structure Considering Electromechanical Characteristics

Kyung-Hun Shin, Tae-Kyoung Bang, Han-Wook Cho, and Jang-Young Choi

***Abstract*—In high-speed permanent magnet synchronous generator (PMSG), the rotor design should not only ensure mechanical stability at high speeds but also ensure the required electromagnetic (EM) performance. This paper deals with the EM analysis and design of high-speed PMSGs considering the rotor structure. In particular, the effects of active power and output voltage due to internal impedance from leakage flux are presented. The relationship between design variables of rotor and performance is analyzed using three-dimensional static finite element analysis and simplified equivalent circuit method. Based on the analysis results, a model with improved EM performance using a nonmagnetic pad is presented according to design parameters of rotor structure. The EM performance and the mechanical reliability of the designed model are validated by comparing the FE results with experimental results.**

***Index Terms*—End effect, electromagnetic analysis, finite element analysis, permanent magnet synchronous generator.**

I. Introduction

HIGH-SPEED permanent magnet synchronous generators (PMSGs) are gaining considerable attention from researchers as well as the industry worldwide owing to their many advantages, such as high efficiency, high power density, simple mechanical construction, no excitation loss, and ease of maintenance [1], [2]. As a result of these advantages, high-speed PMSGs are well-suited for such as home appliances, aerospace technology, marine technology, and flywheel energy storage systems [3]. Despite these advantages as mentioned earlier, the rotor requires a complicated design process using electromechanical analysis in order to secure required electromagnetic (EM) performance and ensure mechanical stiffness for high speed operation [4]–[12].

A high-strength material is used for the shaft coupling component of the PMSG to ensure mechanical rigidity [4], [5]. However, the magnetic properties of the high-strength material can affect EM performance due to leakage flux [10]. The performance of high-speed PMSGs deteriorates due to the increase in the winding reactance and reduction of the flux linkage as a result of end effect [10], [11]. Therefore, it is essential to consider the rotor shaft in the design and analysis of a high-speed PMSG.

This paper deals with how to analyze and improve a problem in which a PMSG does not meet the required active power and output voltage due to an increase in internal impedance of the PMSG with leakage flux of the rotor shaft. The EM analysis was carried out to compare two-dimensional (2D) and 3D models without rotor shaft and 3D models with rotor shaft based on a 2D model that secures required EM performance and satisfies the mechanical requirements. 3D FE analysis was performed to derive the equivalent circuit (EC) parameters according to the design parameters of the rotor shaft. For insight into the relationship between EC parameters and EM performance, the active power and output voltages are analyzed using a simplified EC method. The improved model obtained from the parametric study based on the EM analysis has been validated by the mechanical analysis. The validity of the proposed analysis and design method was verified using experimental results.

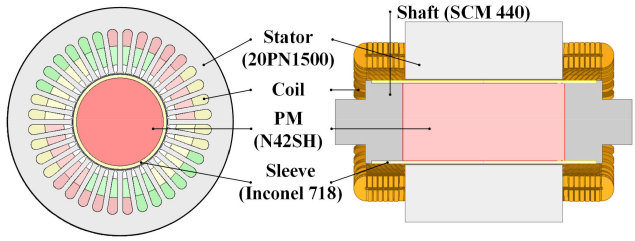

Fig. 1. Schematic of the structure of a high-speed PMSG.

II. Influence of End Effect of High-Speed PMSGs on Electromagnetic Performance

Fig. 1 shows the schematic of the structure of a high-speed PMSG. The PMSG consists of a 36-slots stator with distributed winding and a two-pole parallel-magnetized PM rotor. The PMs are retained within an Inconel 718 sleeve, which has been pressed to the rotor to withstand centrifugal stress under high-speed operating conditions. As previously mentioned, a material (SCM 440) with high strength is used for the shaft coupling component because of the stiffness of the shaft. The specifications and requirements of high-speed PMSGs are listed in Table I.

Manuscript received September 23, 2019; accepted February 19, 2020. Date of publication March 12, 2020; date of current version May 12, 2020. This work was supported by Korea Electric Power Corporation under Grant R18XA06-51. *(Corresponding author: Tae-Kyoung Bang.)*

Kyung-Hun Shin is with the Department of Electrical and Computer Engineering, University of Illinois at Urbana-Champaign, Urbana, IL 61801 USA (e-mail: sinkyunghun@gmail.com).

Tae-Kyoung Bang and Jang-Young Choi are with the Department of Electrical Engineering, Chungnam National University, Daejeon 34134, South Korea (e-mail: bangtk77@cnu.ac.kr; choi_jy@cnu.ac.kr).

Han-Wook Cho is with the Department of Electrical Electronics and Communication Engineering, Chungnam National University, Daejeon 305-764, South Korea (e-mail: hwcho@cnu.ac.kr).

Color versions of one or more of the figures in this article are available online at http://ieeexplore.ieee.org.

Digital Object Identifier 10.1109/TASC.2020.2980536

TABLE I
SPECIFICATIONS OF THE HIGH-SPEED PMSG

Parameters	Values	Parameters	Values
Outer radius of stator	132.5 mm	Inner radius of stator	56.5 mm
Outer radius of PM	51 mm	Thickness of sleeve	4 mm
Stack length of stator	210 mm	Material for stator	25PN1500
Grade of PM	N42SH	Material for sleeve	Inconel718
Slot number	36	Rated speed	15000 rpm
Rated active power	250 kW	Rated voltage	600 V_{rms}

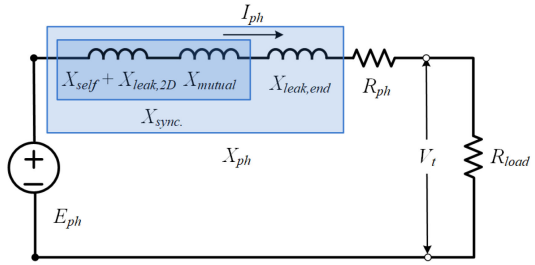

Fig. 2. Equivalent circuit for performance analysis of PMSG.

A. Equivalent Circuit Method

Fig. 2 illustrates the EC of a PMSG for one phase. In the figure, E_{ph} is the open-circuit voltage (back-EMF), V_t is the terminal voltage, I_{ph} is the phase current, R_{ph} is the armature resistance, and X_{ph} is the synchronous reactance [13]. In general, the synchronous reactance includes the self-reactance (X_{self}), the mutual reactance (X_{mutual}), and the leakage reactance (X_{leak}). Furthermore, the leakage reactance can be divided into the slot leakage and the end leakage, and the end leakage is affected by the structure of the rotor shaft.

Assuming that the PMSG operates at a constant speed and unity power factor for resistive loads, the voltage and current of the ECs can be given by (1) and (2) as follows:

$$V_t = E_{ph}\sqrt{\frac{R_{load}^2}{(R_{ph}+R_{load})^2 + (X_{ph})^2}} \tag{1}$$

$$I_{ph} = \frac{E_{ph}}{\sqrt{(R_{ph}+R_{load})^2 + (X_{ph})^2}} \tag{2}$$

where R_{load} is the load resistance and $E_{ph}\ (= K_e\omega)$ is the back-EMF at a given operating speed.

Here, K_e is the back-EMF constant (flux linkage) and ω is the synchronous speed.

Assume that the three phases of the PMSG are balanced and the load resistance has a unity power factor ($\cos\theta = 1$), its active power can be expressed as follows:

$$P_{out} = 3 \cdot V_{t-rms} \cdot I_{ph-rms} \cdot \cos\theta \tag{3}$$

where V_{t-rms} and I_{ph-rms} are root mean square (rms) values of terminal voltage and current. From (1)–(3), the load resistances that gives the rated active power can be determined as follows:

$$R_{load}^{rated} = \frac{3E_{ph}^2 \pm \delta - 2P_{out}^{rated}R_{ph}}{2P_{out}^{rated}} \tag{4}$$

$$\delta = \sqrt{\left(3E_{ph}^2\right)^2 - 12R_{ph}P_{out}^{rated}E_{ph}^2 - 4\left(P_{out}^{rated}\right)^2 X_{ph}} \tag{5}$$

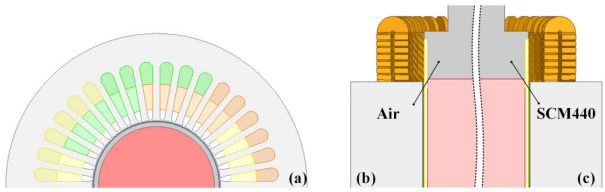

Fig. 3. Analysis model: (a) 2D FE model, (b) 3D FE model without shaft (3D FE-1), and (c) 3D FE model with shaft (3D FE-2).

TABLE II
2D AND 3D FE STATIC ANALYSIS RESULTS WITH/WITHOUT ROTOR SHAFT

Description	Unit	Value		
		2D FE	3D FE-1	3D FE-2
Flux linkage	Wb	0.340	0.363	0.344
Inductance	μH	229.8	353.1	475
Resistance	mΩ	10.2		

It is clear from the EC method that the back-EMF, the phase resistance, and the synchronous reactance are parameters that influence the performance of the PMSG. Therefore, accurate prediction of EC parameters is very important for EM analysis.

B. Influence of Rotor Shaft on Electromagnetic Performance

In general, 2D FE analysis can be performed within a few hours. Nevertheless, 3D FE analysis involves a large number of meshes; thus, a considerable amount of time is required to analyze the machine performance.

In addition, performance analysis of PMSG requires more time as the transient analysis process requires a combination of both the EM field and the electric circuit. To overcome these problems, the flux linkage and synchronous inductance were calculated in this study using static 3D FE analysis, whereas the phase resistances were calculated in [11]. 3D leakage effects in PMSGs with/without rotor shaft can be determined using both 2D and 3D FE analyses by calculating the flux linkages and inductances for different shaft geometries, as shown in Fig. 3. The EC parameters obtained from 2D and 3D FE analyses with/without shaft are listed in Table II.The flux linkage obtained using 3D analysis approach is higher than that of 2D analysis approach due to PM overhang [11]. Although the total flux increased due to PM overhang, 3D analysis result considering rotor shaft shows that the flux linkage is similar to that of 2D analysis result due to the leakage flux.

In particular, it was observed that the leakage inductance of the stator coil significantly increased as a result of the end effect with the rotor shaft. Consequently, an increase in the reactance due to leakage inductance causes a decrease in the active power owing to reactance voltage drop. As shown in Fig. 4, 2D and 3D analyses without rotor shaft yielded an active power of over 250 kW at rated voltage of 600 V. In contrast, the active power obtained from 3D analysis with rotor shaft is lower than 250 kW at rated voltage.

In order to verify the validity of the proposed analysis method, the results of 3D FE analysis considering loss and saturation at rated voltage are presented in Table III. Compared with the proposed method, the active power analysis results obtained from the FE analysis under the same load resistance conditions are 2% (2D FE), 4.23% (3D FE-1), and 4.56% (3D FE-2),

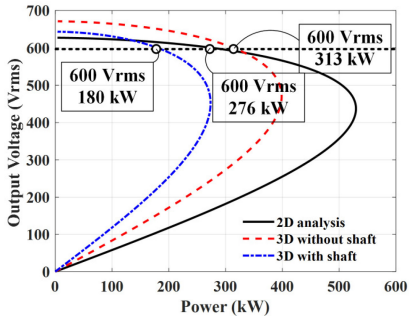

Fig. 4. Generating characteristic analysis for AC load condition at 15,000 rpm.

TABLE III
2D AND 3D FE TRANSIENT ANALYSIS RESULTS WITH/WITHOUT ROTOR SHAFT UNDER LOAD CONDITION

Description	Unit	Value		
		2D FE	3D FE-1	3D FE-2
Output voltage	V	606.25	582.37	612.04
Active power	kW	281.64	294.89	212.09
Copper loss	kW	2.20	2.62	1.20
Core loss	kW	0.91	0.83	0.90
Eddy current loss	kW	0.56	0.28	0.21

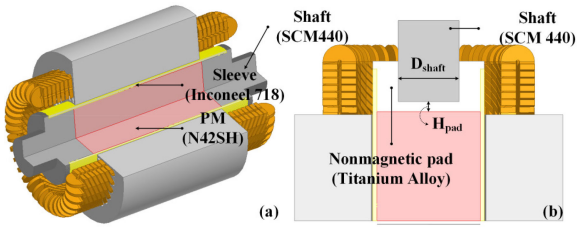

Fig. 5. (a) 3D structure of PMSG with shaft and (b) design variables.

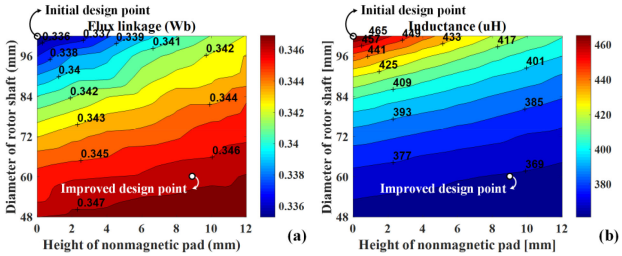

Fig. 6. Analysis results considering the height of the nonmagnetic pad (H_{pad}) and diameter of the rotor shaft (D_{shaft}): (a) flux linkage and (b) inductance.

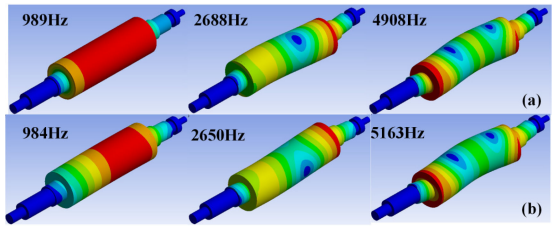

Fig. 7. Modal analysis: (a) initial and (b) improved rotor.

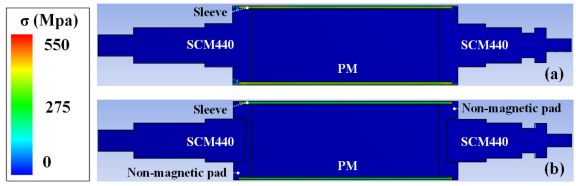

Fig. 8. Stress analysis results: (a) initial and (b) improved rotor.

respectively. Because high-speed PMSG has a high operating frequency, the saturation of the stator is taken into account at the design stage, and the error between the FE method and the EC method is reasonable because the ratio of copper loss to the total loss ratio is large. Therefore, it is considered that the proposed analysis method can be usefully used in the design stage that requires a lot of analysis.

C. Parametric Analysis for Improving EM Performance Considering Design Variables of the Rotor Shaft

It can be observed that the EM performance is significantly affected by 3D leakage flux effect. Therefore, EM performance analysis of high-speed PMSGs was carried out considering the 3D structure and the design parameters of the rotor shaft were defined, as shown in Fig. 5. In order to secure the mechanical stiffness, a nonmagnetic pad was used with titanium alloy and the mechanical stability was verified through structural analysis.

Fig. 6 shows variations in the flux linkage and inductance values for different non-magnetic pad thicknesses (H_{pad}) and shaft outer diameter values (D_{shaft}). The objective of the improved design is to improve the active power, to meet the required performance that over the output power of 250 kW when the rated voltage of 600 V_{rms} is satisfied.

III. VERIFICATION OF ROTOR DESIGN USING MECHANICAL ANALYSIS

Despite improvement in the EM performance, the combination of two different objects can deteriorate the mechanical properties.

Therefore, mechanical analysis of an electromagnetically improved rotor is essential. The validity of the proposed design method was verified through mechanical analysis of the improved model using an initial model. Mechanical analysis can be divided into modal analysis to predict the natural frequency [7], stress analysis between the rotor PM and the sleeve [4], [6], [7], and rotor dynamics analysis [12].

Fig. 7 shows the first, second, and third mode shapes obtained from the modal analysis of the initial and improved models. At the rated speed of 15,000 rpm, the fundamental frequency of the PMSG is 250 Hz, and the modal analysis of the initial and improved models shows that there is no match at any harmonic frequency.

The safety factor (yield strength/maximum stress) of the PM and sleeve is required to be at least 1 [4], [14]. Especially in the case of high speed PMSGs, it is required to secure a high safety factor because the reliability of the rotor is required at high rotational speeds. Fig. 8 shows the stress analysis results of the initial and the improved rotor. According to the material properties as shown in Table IV and rated speed conditions, the safety factors of the PM and the sleeve of the two models are

TABLE IV
MATERIAL PROPERTIES FOR ROTOR STRUCTURE

Material \ Description	Density [kg/m^3]	Poisson's ratio	Young's modulus [GPa]	Yield strength [MPa]
Sm_2Co_{17}	8,300	0.24	120	35
Inconel 718	8,190	0.284	205	1,100
SCM440	7,850	0.29	205	675
Titanium alloy	4,400	0.33	114	820

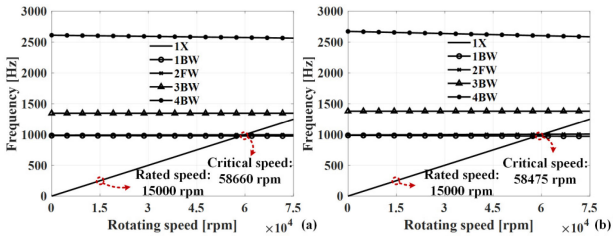

Fig. 9. Campbell diagram: (a) initial and (b) improved design.

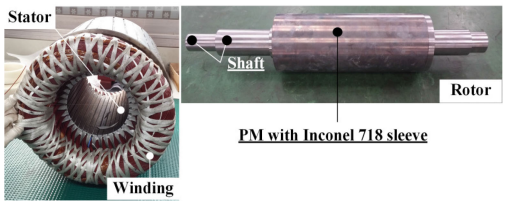

Fig. 10. Manufactured high-speed PMSG.

more than 2.5, indicating that it is mechanically stable. Similarly, the safety factor of the rotor structure (SCM 440 and Titanium alloy) also has a value greater than 2.

Finally, the mechanical speed of the high-speed PMSG is limited by the critical speed [12]. As shown in Fig. 9, the rated speed of the initial and improved models is sufficiently low compared with the critical speed. It can be seen that the critical speed is similar to the initial design in the rated operating conditions despite the change in the material and design of the rotor structure.

From the analysis results, it can be observed that the improved model has stable mechanical properties without problems such as bearing fatigue failure and rubbing.

IV. EXPERIMENTAL RESULTS AND DISCUSSIONS

The improved design model based on electro-mechanical analysis results was manufactured, as shown in Fig. 10. The improved rotor structure that ensures mechanical stability has a non-magnetic pad thickness and a rotor shaft diameter of 9 mm and 60 mm, respectively.

Table V presents the analysis and measurement results of the EC parameters of the improved design and prototype. The analysis results of the flux linkage and inductance of the high-speed PMSG considering the rotor shaft are in good agreement with measured results; the errors are 0.3% and 4%, respectively. An experimental setup was constructed to verify the validity of the proposed design and the analysis method, as shown in Fig. 11. The drive motor provides a constant speed and the input

TABLE V
IMPROVED AND MEASURED VALUES OF HIGH-SPEED PMSG

Description	Unit	Value	
		Improved	Meas.
Flux linkage	Wb	0.358	0.359
Inductance	μH	368.3	354
Resistance	mΩ	10.2	10.82

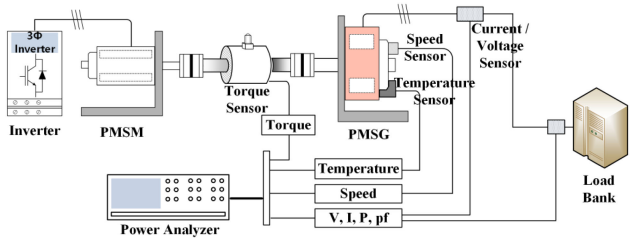

Fig. 11. Experimental setup.

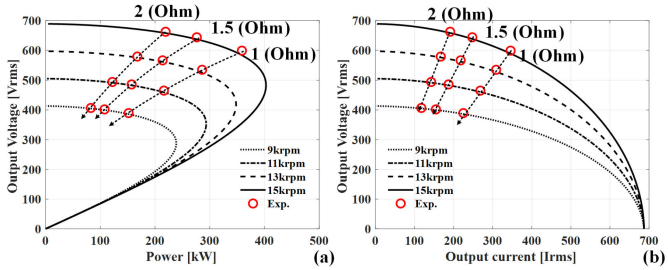

Fig. 12. Generating characteristics at different AC load and rotor speed conditions: (a) power–voltage curve and (b) current–voltage curve.

power was determined by the load of the PMSG. To evaluate the output of the PMSG itself, the EM performance can be measured by connecting the resistance of each phase to the wye connection. The results of the generating characteristic of the improved model and the prototype at different load resistances and operating speeds are shown in Fig. 12.

The error of the measurement results is within 5% of the analysis results. From the results, it can be confirmed that the analysis and design results presented in this paper are reliable even under various load resistance and speed conditions.

V. CONCLUSION

This paper presents the electro-mechanical performance analysis and design method of a PMSG considering the rotor shaft. Compared with 2D FE analysis results, results of 3D FE analysis with rotor shaft show a decrease in the back-EMF and an increase in the leakage inductance, which can be attributed to performance deterioration. Therefore, the EM parameter map was derived based on the design parameters of the rotor shaft using 3D FE static analysis and the performance of the high-speed PMSG was analyzed using the EC method. Mechanical analyzes were performed to verify the mechanical reliability of the optimized rotor shaft. The validity of the proposed design and analysis results was verified using experimental results. The proposed method can be used for the design and analysis of high-speed electrical machines.

REFERENCES

[1] D.-K. Hong, D. Joo, B.-C. Woo, Y.-H. Jeong, and D.-H. Koo, "Investigations on a super high speed motor-generator for microturbine applications using amorphous core," *IEEE Trans. Magn.*, vol. 49, no. 7, pp. 4072–4075, Jul. 2013.

[2] X. Liu, G. Liu and B. Han, "A loss separation method of a high-speed magnetic levitated PMSM based on drag system experiment without torque meter," *IEEE Trans. Ind. Electron.*, vol. 66, no. 4, pp. 2976–2986, Apr. 2019.

[3] X. Zhang and J. Yang, "A DC-link voltage fast control strategy for high-speed PMSM/G in flywheel energy storage system," *IEEE Trans. Ind. Appl.*, vol. 54, no. 2, pp. 1671–1679, Mar./Apr. 2018.

[4] J.-H. Ahn, C. Han, C.-W. Kim, and J.-Y. Choi, "Rotor design of high speed permanent magnet synchronous motors considering rotor magnet and sleeve materials," *IEEE Trans. Appl. Supercond.*, vol. 28, no. 3, Apr. 2018. Art. no. 5201504.

[5] D.-H. Jung, J.-K. Lee, J.-Y. Kim, I. S. Jang, J. Lee, and H.-J. Lee, "Design method of an ultrahigh speed PM motor/generator for electric turbo compounding system," *IEEE Trans. Appl. Supercond.*, vol. 28, no. 3, Apr. 2018. Art. no. 5202804.

[6] J. H. Ahn, J. Y. Choi, C. H. Park, C. H, C. W. Kim, and T. G. Yoon, "Correlation between rotor vibration and mechanical stress in ultra-high speed permanent magnet synchronous motors," *IEEE Trans. Magn.*, vol. 53, no. 11, Nov. 2017, Art. no. 8209906.

[7] Z. Huang and J. Fang, "Multiphysics design and optimization of high speed permanent-magnet electrical machines for air blower applications," *IEEE Trans. Ind. Electron.*, vol. 63, no. 5, pp. 2766–2774, May 2016.

[8] N. Uzhegov, A. Smirnov, C. H. Park, J. H. Ahn, J. Heikkinen, and J. Pyrhönen, "Design aspects of high-speed electrical machines with active magnetic bearings for compressor applications," *IEEE Trans. Ind. Electron.*, vol. 64, no. 11, pp. 8427–8436, Nov. 2017.

[9] M. S. Barrans, M. M. J. Al-Ani, and J. Carter, "Mechanical design of rotors for permanent magnet high speed electric motors for turbocharger applications," *IET Elect. Syst. Transp.*, vol. 7, no. 4, pp. 278–286, 2017.

[10] M. F. Hsieh, Y. C. Hsu, D. G. Dorell, and K. H. Hu, "Investigation on end winding inductance in motor stator windings," *IEEE Trans. Magn.*, vol. 43, no. 6, pp. 2513–2515, Jun. 2007.

[11] J. J. Potgieter and M. J. Kamper, "Calculation methods and effects of end-winding inductance and permanent-magnet end flux on performance prediction of nonoverlap winding permanent-magnet machines," *IEEE Trans. Ind. Appl.*, vol. 50, no. 4, pp. 2458–2466, Jul./Aug. 2014.

[12] G. H. Jang, J. H. Ahn, B. O. Kim, D. H. Lee, J. S. Bang and J. Y. Choi, "Design and characteristic analysis of a high-speed permanent magnet synchronous motor considering the mechanical structure for high-ppeed and high-head centrifugal pumps," *IEEE Trans. Magn.*, vol. 54, no. 11, Nov. 2018, Art. no. 8204906.

[13] K.-H. Shin, K.-H. Jung, H.-W. Cho, and J.-Y. Choi, "Analytical modeling and experimental verification for electromagnetic analysis of tubular linear synchronous machines with axially magnetized permanent magnets and flux-passing iron poles," *IEEE Trans. Magn.*, vol. 54, no. 11, Nov. 2018, Art. no. 8204006.

[14] R. G. Budynas, *Advanced Strength and Applied Stress Analysis*, NewYork, NY, USA: McGraw-Hill, 1998, p. 960.